

BRL

AD 1463

REPORT NO. 1463

NEGATIVE ION REACTIONS IN NO-H₂O MIXTURES

by

L. J. Puckett
W. C. Lineberger

December 1969

This document has been approved for public release and sale;
its distribution is unlimited.

U.S. ARMY ABERDEEN RESEARCH AND DEVELOPMENT CENTER
BALLISTIC RESEARCH LABORATORIES
ABERDEEN PROVING GROUND, MARYLAND

Destroy this report when it is no longer needed.
Do not return it to the originator.

The findings in this report are not to be construed as
an official Department of the Army position, unless
so designated by other authorized documents.

BALLISTIC RESEARCH LABORATORIES

REPORT NO. 1463

DECEMBER 1969

NEGATIVE ION REACTIONS IN NO-H₂O MIXTURES

L. J. Puckett

W. C. Lineberger

Signature and Propagation Laboratory

This document has been approved for public release and sale;
its distribution is unlimited.

1
:
1 7, 1969, 11: 01003

RDT&E Project No. 5910.21.61160

ABERDEEN PROVING GROUND, MARYLAND

BALLISTIC RESEARCH LABORATORIES

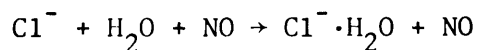
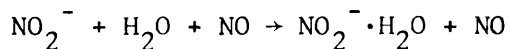
Report No. 1463

LJPuckett/WCLineberger†/n11
 Aberdeen Proving Ground, Md.
 December 1969

NEGATIVE ION REACTIONS IN NO-H₂O MIXTURES*

ABSTRACT

A stationary afterglow system has been utilized to determine rate constants for thermal energy negative ion-molecule reactions in photo-ionized NO-H₂O mixtures. When the decay of the plasma is controlled by ambipolar diffusion of positive and negative ions quantitative determination of rate constants is shown to be feasible. The plasma transition from electron-positive ion ambipolar diffusive domination of the transport loss processes to domination by positive ion-negative ion ambipolar diffusion is explained by a model which includes the effects of negative ion trapping. Prominent negative ions in the afterglow include NO₂⁻, its hydrates, and clusters involving HNO₂. Reaction rate constants for the processes



are found to be $1.3 \pm 0.3 \times 10^{-28} \text{ cm}^6/\text{sec}$ and $3.4 \pm 1.3 \times 10^{-29} \text{ cm}^6/\text{sec}$ at 293 K, respectively. Steady glows in NO-H₂O-O₂ mixtures revealed that NO₃⁻ and the impurity HCO₃⁻ also formed multiple hydrates and clustered with HNO₂. These results indicate that the terminal negative ions in the D-region of

the ionosphere will likely be hydrated.

* Research supported in part by Defense Atomic Support Agency

† Present Address: Joint Institute for Laboratory Astrophysics
University of Colorado
Boulder, Colorado 80302

TABLE OF CONTENTS

	Page
ABSTRACT	3
LIST OF ILLUSTRATIONS	7
I. INTRODUCTION	9
II. EXPERIMENTAL APPARATUS AND PROCEDURES	10
III. AFTERGLOW ANALYSIS	12
IV. EXPERIMENTAL RESULTS ANALYSIS AND DISCUSSION	17
DISTRIBUTION LIST	27

LIST OF ILLUSTRATIONS

Figure	Page
1. Schematic diagram of stationary afterglow apparatus . . .	11
2. Temporal afterglow profiles of NO^+ , $\text{NO}^+\cdot\text{NO}$ and NO_2^- wall currents at 50 mTorr NO pressure	13
3. Evolution of the negative ion spectrum as a function of increasing H_2O concentration in NO at 400 mTorr NO pressure. The integrated spectrum for each H_2O concentration is normalized to the same value . ²	18
4. Variation of NO_2^- reactive loss frequency as a function of the product of NO and H_2O pressures	22
5. Negative ion spectrum in 200 mTorr NO, 5 mTorr H_2O and 5 mTorr O_2	23

I. INTRODUCTION

Recently Lineberger and Puckett^{1,2*} reported stationary afterglow measurements of NO^+ reactions leading to the formation of $\text{NO}^+\cdot\text{NO}$, $\text{NO}^+\cdot n(\text{H}_2\text{O})$ and $\text{H}_3\text{O}^+\cdot n(\text{H}_2\text{O})$ ions in photoionized $\text{NO}-\text{H}_2\text{O}$ mixtures. These investigations elucidated a mechanism by which NO^+ ions can be lost in reactions with atmospheric water vapor. As a consequence of these reactions it is understandable that NO^+ should not be regarded as a terminal positive ion in the D-region of the ionosphere.

Ferguson³ and LeLevier and Branscomb⁴ have reviewed D-region negative ion chemistry and **concluded that the "terminal" negative ions are NO_2^- and NO_3^-** . This conclusion was based on the observation that these ions are formed through chain-breaking reactions that do not permit the electron to be freed again. Therefore, in their context, "terminal" implies that the ions are indestructable except through ion-ion mutual neutralization processes. We report results which demonstrate that both NO_2^- and NO_3^- ions do, however, undergo clustering reactions with H_2O and HNO_2 at 293 K.

The negative ion-molecule reaction rate constants reported in this paper are the first such measurements known to the authors to be made using stationary afterglow techniques. In order to obtain quantitative negative ion reaction rate information from a stationary afterglow, it is necessary to make observations subsequent to the disappearance of electrons from the decaying plasma during the interval when positive

*References are listed on page 25.

ion-negative ion ambipolar diffusion is the dominant transport loss mechanism. The transition from positive ion-electron ambipolar diffusive domination to positive ion-negative ion ambipolar diffusive domination is marked by a sudden increase in the negative ion wall current, and a sudden decrease in the positive ion wall current. A model is presented which accounts for the features of this transition.

II. EXPERIMENTAL APPARATUS AND PROCEDURES

The basic apparatus employed in this experiment is the photoionized-stationary-afterglow instrument described previously¹ and only a brief account of the apparatus will be presented here. For the present work the mass filter was modified to permit observation of negative ions. A schematic diagram of the apparatus is shown in Fig. 1.

The afterglow cavity is an ultra-high-vacuum, bakeable, gold-coated-stainless-steel cylinder 18 inches in diameter and 36 inches long. Information on the individual ion species in the plasma afterglow is obtained by means of time-resolved mass spectrometry of the ions which pass through a 0.60 mm diameter sampling orifice in the cavity wall. The sampling orifice is contained in a plate which is contoured to the shape of the cavity wall and electrically insulated from the wall. The potential on the plate is set at a variable but low attractive potential (<100mV). The orifice plate potential did not effect the rate constant determinations in this work; however, we have noted¹ that observed diffusion loss rates are affected by the plate potential. Consequently, care must be exercised in all measurements of diffusion coefficients in cases where draw-out

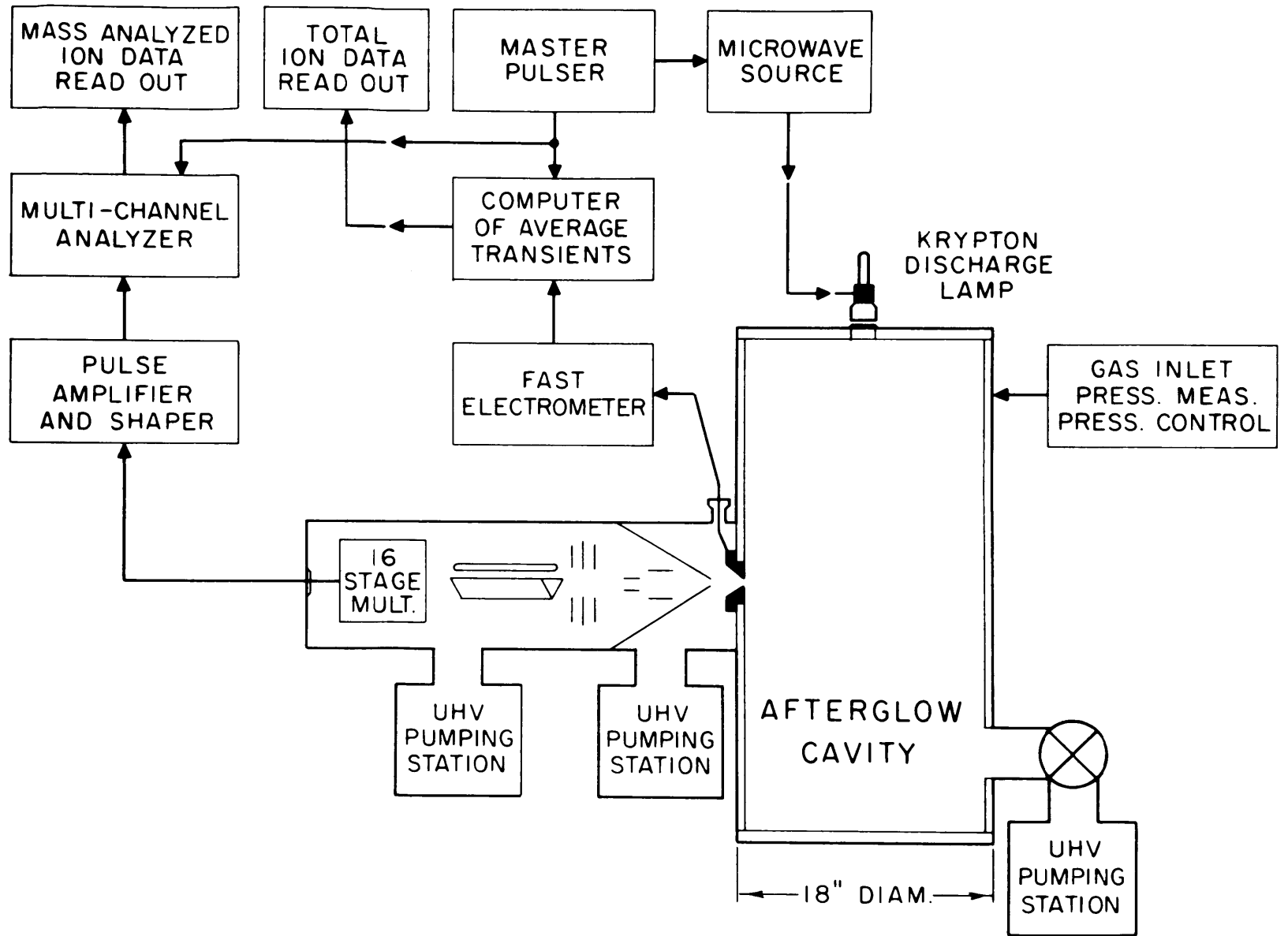


Figure 1. Schematic diagram of stationary afterglow apparatus

potentials are employed.

In this investigation the negative ions were formed by electron attachment in the gas. The electrons were produced by photoionization of NO by means of krypton resonance radiation (123.6 and 116.5 nm) from a pulsed microwave-powered discharge lamp. Initial ion density is sufficiently low ($\sim 10^6 \text{ cm}^{-3}$) that recombination loss rates are negligible compared with reactive and diffusive loss rates.

The NO gas used in this work was processed in the following manner. Specially prepared gas of 99.9 per cent stated purity was obtained from a steel cylinder. The gas was passed through a stainless steel and glass line to a LN_2 trap where it was condensed. By means of a refrigerating vapor bath⁵ the trap temperature could be maintained within ± 1.0 K of any desired temperature in the range 77 to ~ 300 K. The NO vapor at the selected trap temperature was passed through a servo-controlled leak valve to the afterglow chamber. The experimental results in this paper were found to be insensitive to trap temperatures below ~ 200 K. Above this temperature trace amounts of NO_2 in the NO were not completely trapped and appeared as impurity ions in the afterglow. Water vapor densities required for the rate constant determinations were obtained in the manner described previously².

III. AFTERGLOW ANALYSIS

Fig. 2 shows the temporal profiles of the principal positive and negative ions in a photoionized NO afterglow at a total pressure of 50 mTorr. The primary ion NO^+ and its termolecular reaction to form $\text{NO}^+ \cdot \text{NO}$

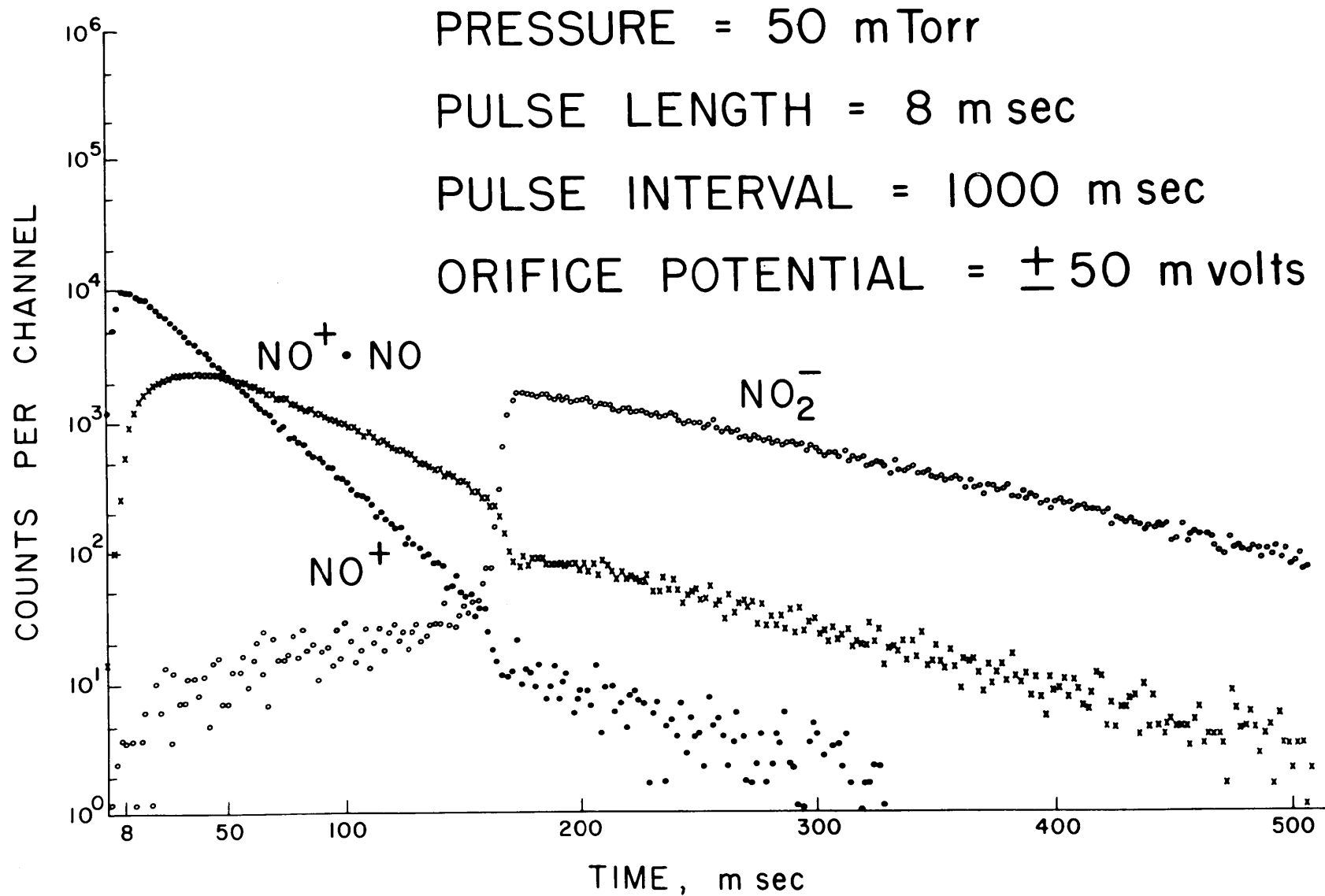


Figure 2. Temporal afterglow profiles of NO⁺, NO⁺·NO and NO₂⁻ wall currents at 50 mTorr NO pressure

have been discussed previously¹. The principal negative ion observed was NO_2^- . The initial formation mechanism for NO_2^- is currently under investigation and will be reported in a future publication.

The temporal profiles in Fig. 2 show marked transitions in positive and negative ion behavior at ~ 170 msec. The transitions in the ion currents to the wall are associated with the transition in volume transport from electron-ion ambipolar diffusive domination to positive ion-negative ion ambipolar diffusive domination, and the resulting release of trapped negative ions. The trapping of negative ions prior to this transition, coupled with sampling discrimination effects, have thwarted previous efforts⁶ to measure negative ion-molecule reaction rates in stationary afterglow experiments. In order to establish the validity of the reaction rate data presented here, it is necessary to investigate and explain the features of the transition. This section is accordingly devoted to an analysis of the plasma decay for times before, during, and after the transition.

In Fig. 2, for times < 170 msec, the positive ion decays are completely explained¹ by interconversion and positive ion-electron ambipolar diffusive⁷ loss. The principal features of the plasma decay that remain to be explained are as follows:

1. The negative ion wall current increases sharply at 170 msec and then decays exponentially.
2. All ions decay exponentially with the same time constant after 170 msec.
3. Both of the positive ion wall currents exhibit a sudden decrease

by approximately a factor of two at 170 msec.

These features are all quantitatively explained in the context of a simple ambipolar diffusion model, as outlined below. The diffusion current density, Γ , of positive ions, negative ions and electrons in the afterglow may be expressed by⁷

$$\Gamma_+ = -D_+ \nabla N_+ + N_+ \mu_+ E \quad (1)$$

$$\Gamma_- = -D_- \nabla N_- - N_- \mu_- E \quad (2)$$

and

$$\Gamma_e = -D_e \nabla N_e - N_e \mu_e E \quad (3)$$

respectively. The quantities D_i and μ_i are free diffusion coefficients and mobilities, while E is the electric field produced by non-charge neutrality in the plasma. The free diffusion term, $-D_i \nabla N_i$, is due to the density gradient of the i th charged species, while the mobility term, $N_i \mu_i E$, describes the field induced charged particle drift in the gas. Although there are no applied electric fields in the afterglow, a "self-field" develops due to the initial rapid diffusion of electrons, producing a net charge separation which retards electron diffusion and enhances positive ion diffusion. It may be shown⁷ using the Einstein relation, $\mu = \frac{eD}{kT}$, that the free diffusion terms and the mobility terms are of equal magnitudes. For positive ions the mobility term produces a current in the same direction as that of free diffusion.

Hence,
$$\Gamma_+ = -2D_{+,e} \nabla N_+ \equiv -D_{+,e} \nabla N_+, \quad (4)$$

where $D_{+,e}$ is defined as the positive ion-electron ambipolar diffusion coefficient, and is equal to twice the free diffusion coefficient, D_+ .

In the case of electrons, the free diffusion coefficient, D_e , and the mobility, μ_e , are a factor of 10^5 greater than those corresponding

to ions in the afterglow. In spite of the fact that diffusion and mobility terms are in opposition for electrons, these terms are of sufficient magnitude such that a departure of about 1 part in 10^5 from complete cancellation is adequate to maintain $\Gamma_e = \Gamma_+$.

In addition to being lost through positive ion-electron diffusion, electrons are lost in attaching reactions which form negative ions. The electric field opposes the radial diffusion of negative ions, however, and as a result

$$\Gamma_- \approx 0, \quad (5)$$

as can be seen in Fig. 2 for $t < 170$ msec. In this sense the negative ions are trapped in the afterglow. Thus, the plasma decays through positive ion-electron ambipolar diffusion until the number density of electrons is no longer sufficient to maintain the electric field which gave rise to ambipolar diffusion and negative ion containment. The collapse of the electric field in the plasma is evidenced in the afterglow profile at ≈ 170 msec. According to Eq.(3), in the absence of the electric field, $\Gamma_e = -D_e \nabla N_e$ and the remaining electrons are lost very rapidly by free diffusive processes. In this simple model the positive ion diffusion current Γ_+ decreases from $2D_+ \nabla N_+$ to $D_+ \nabla N_+$, which gives rise to a rapid drop of wall current by a factor of two followed by a continued reduction by a factor of two in the exponential rate of plasma decay. Both of these features are apparent in the afterglow profile. The collapse of the E-field also terminates the containment of the negative ions in the afterglow and produces a rapid increase of Γ_- from ≈ 0 to the value $\Gamma_- = -D \nabla N_-$, which in the first approximation is equal Γ_+ . These characteristics in the negative ion behavior are also observable in the afterglow profile.

The relatively simple model described above qualitatively accounts for all of the observed transition features. A more refined numerical analysis of the transition, involving only the assumption of charge neutrality, has recently been completed by Kregel⁸. This more refined calculation reproduces both the observed buildup of negative ion current prior to the transition, and the smoothing of the transition observed in the positive ion wall current.

IV. EXPERIMENTAL RESULTS AND DISCUSSION

These measurements are believed to constitute the first measurements of negative ion reaction rate constants to be obtained with a stationary afterglow apparatus. Negative ions have been observed in other stationary afterglow experiments⁶, but because of small signals and ion discrimination effects, the previous observations were unable to follow the afterglow into the positive ion-negative ion ambipolar diffusion regime. Consequently for all times during the observations⁶ there were both negative ion sources which were difficult to evaluate and non-equilibrium ionic spatial distributions. As a result of these conditions meaningful negative ion reaction rate constants could not be obtained.

With the apparatus employed in this work the afterglow has been observed over seven decades of decay, four decades of which followed the electron-ion to ion-ion transition, i.e. four decades of decay in which there were negligible net sources of negative ions, and the ionic spatial distribution was a fundamental mode diffusive distribution.

Fig. 3 shows the negative ion spectrum in pure nitric oxide and in

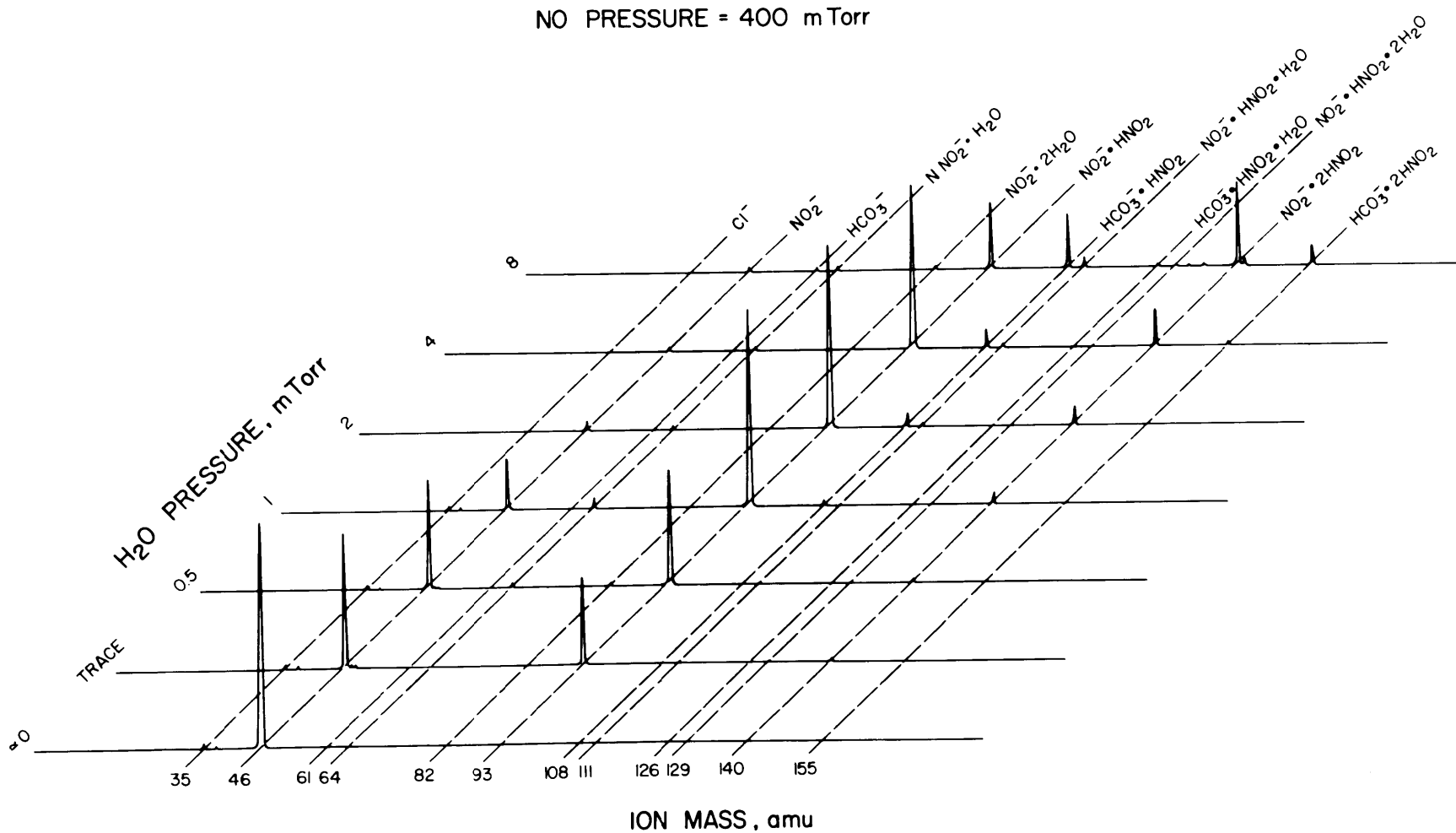
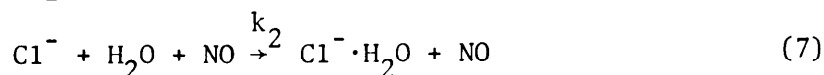
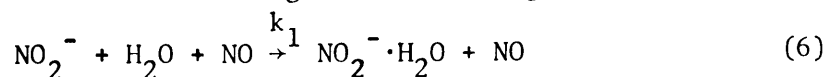


Figure 3. Evolution of the negative ion spectrum as a function of increasing H₂O concentration in NO at 400 mTorr NO pressure. The integrated spectrum for each H₂O concentration is normalized to the same value

nitric oxide with varying amounts of water vapor. The dominant ion is NO_2^- followed in intensity by Cl^- . (The Cl probably originates in the AgCl cement used to attach the MgF_2 windows to the afterglow chamber.) In pure NO, NO_2^- is the dominant negative ion throughout the afterglow; however, when H_2O is added in small amounts other ions become prominent. Principal among these ions is $\text{NO}_2^- \cdot \text{HNO}_2$. Clusters of NO_2^- with H_2O become increasingly important as the water vapor pressure increases. The hydrated NO_2^- and Cl^- are formed through the following reactions:



The rate constants k_1 and k_2 can be deduced through the following analysis.

If there are no NO_2^- sources and the dominant loss processes for NO_2^- ions in dilute H_2O -NO mixtures are positive ion-negative ion ambipolar diffusion and the reaction represented by Eq.(6), then for a fundamental mode diffusive distribution in a cylindrical cavity of radius R cm, the NO_2^- density in the afterglow may be expressed as

$$[\text{NO}_2^-(r,t)] = [\text{NO}_2^-(o,T)] J_0(2.405r/R) \cdot \exp\left\{-\left(\frac{D_{+,-}}{\Lambda^2}\right) - k_1[\text{NO}][\text{H}_2\text{O}]\right\}(t-T), \quad (8)$$

which is valid for $t > T$. Brackets, [], denote the number density in cm^{-3} , $[\text{NO}_2^-(o,T)]$ is the axial number density at the time, T, of the transition from electron-ion to ion-ion ambipolar diffusion domination, and Λ is the characteristic diffusion length of the afterglow chamber.

It can be shown that under the proper experimental conditions¹, the count rate of a mass-analyzed ionic species is directly proportional to the ionic volume number density of that species. If the reciprocal time

constant for the observed decay of NO_2^- is denoted by ν , then

$$\nu = \frac{D_{+,-}}{\Lambda^2} + k_1 [\text{NO}] [\text{H}_2\text{O}] \quad (9)$$

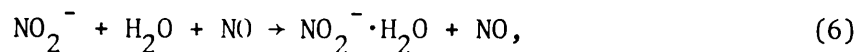
When trace amounts of H_2O are added to the NO , $\frac{D_{+,-}}{\Lambda^2}$ is not significantly affected and the contribution of $k_1 [\text{NO}] [\text{H}_2\text{O}]$ to ν can be measured. A plot of $\nu - \frac{D_{+,-}}{\Lambda^2}$ as a function of $[\text{NO}] [\text{H}_2\text{O}]$ will indicate the dependence of the reaction on the NO and H_2O concentrations, and from this information the rate constant k_1 can be evaluated. The experimental data shown in Fig. 4 yield a value of $k_1 = 1.3 \pm 0.3 \times 10^{-28} \text{ cm}^6/\text{sec}$. Employing the same analysis for the Cl^- reactions as that described for NO_2^- the rate constant for the hydration of Cl^- , Eq. (7), was determined to be $k_2 = 3.4 \pm 1.3 \times 10^{-29} \text{ cm}^6/\text{sec}$. In order to deduce the sequence of reactions which produce the prominent ion, $\text{NO}_2^- \cdot \text{HNO}_2$, the following observations were made:

1. The NO_2^- count rate did not vary with either irradiation time (for times \gg the characteristic lifetime of the ion in the system) or with the residence time of gas in the chamber.
2. The count rate of $\text{NO}_2^- \cdot \text{HNO}_2$, however, did increase as a function of irradiation time, but did not increase with residence time of the gas in the chamber.

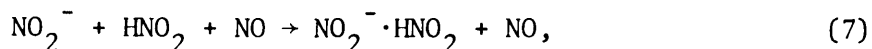
Observations 1 and 2, together, indicate that the reactant HNO_2 was produced through radiation chemistry. This conclusion is in accord with previous investigations² which delineated a source of HNO_2 through $\text{NO}^+ - \text{H}_2\text{O}$ gas phase chemistry.

3. The exponential decay of $\text{NO}_2^- \cdot \text{HNO}_2$ in the afterglow is substantially slower than that of NO_2^- , and lends further support to the conclusion that $\text{NO}_2^- \cdot \text{HNO}$ is not produced in reactions of NO_2^- with the

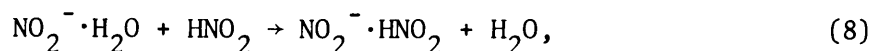
chamber walls, but rather in gas phase reactions. Fig. 4 of this paper reveals, however, that the dominant loss of NO_2^- in $\text{NO-H}_2\text{O}$ mixtures is the reaction



and not directly through



eventhough Fig. 3 indicates that the abundance of $\text{NO}_2^- \cdot \text{HNO}_2$ greatly exceeds that of $\text{NO}_2^- \cdot \text{H}_2\text{O}$. The indicated conclusion is therefore, that the principal source of $\text{NO}_2^- \cdot \text{HNO}_2$ is the reaction



with reaction (7) being a minor source of $\text{NO}_2^- \cdot \text{HNO}_2$ under the conditions of this investigation. Reaction (8) is an example of the "switching" reactions recently reported by Adams et al⁹, and the fact that reaction (8) is rapid indicates that the $\text{NO}_2^- \cdot \text{HNO}_2$ bond strength is greater than the $\text{NO}_2^- \cdot \text{H}_2\text{O}$ bond strength.

At the higher H_2O concentrations in Fig. 3 clustering reactions with both H_2O and HNO_2 prevail and the final negative ions are considerably more complex than NO_2^- . Similarly, clusters of the impurity, HCO_3^- , were observed to account for a large portion of the total ion spectrum at the higher water concentrations shown in Fig. 3. Further investigations revealed that NO_3^- present in $\text{NO-H}_2\text{O-O}_2$ mixtures (Fig. 5) also clustered with H_2O and HNO_2 . In this figure tentative identifications are made based on mass-to-charge ratios.

The present findings serve to indicate that those ions previously designated as terminal negative ions in the D-region of the ionosphere

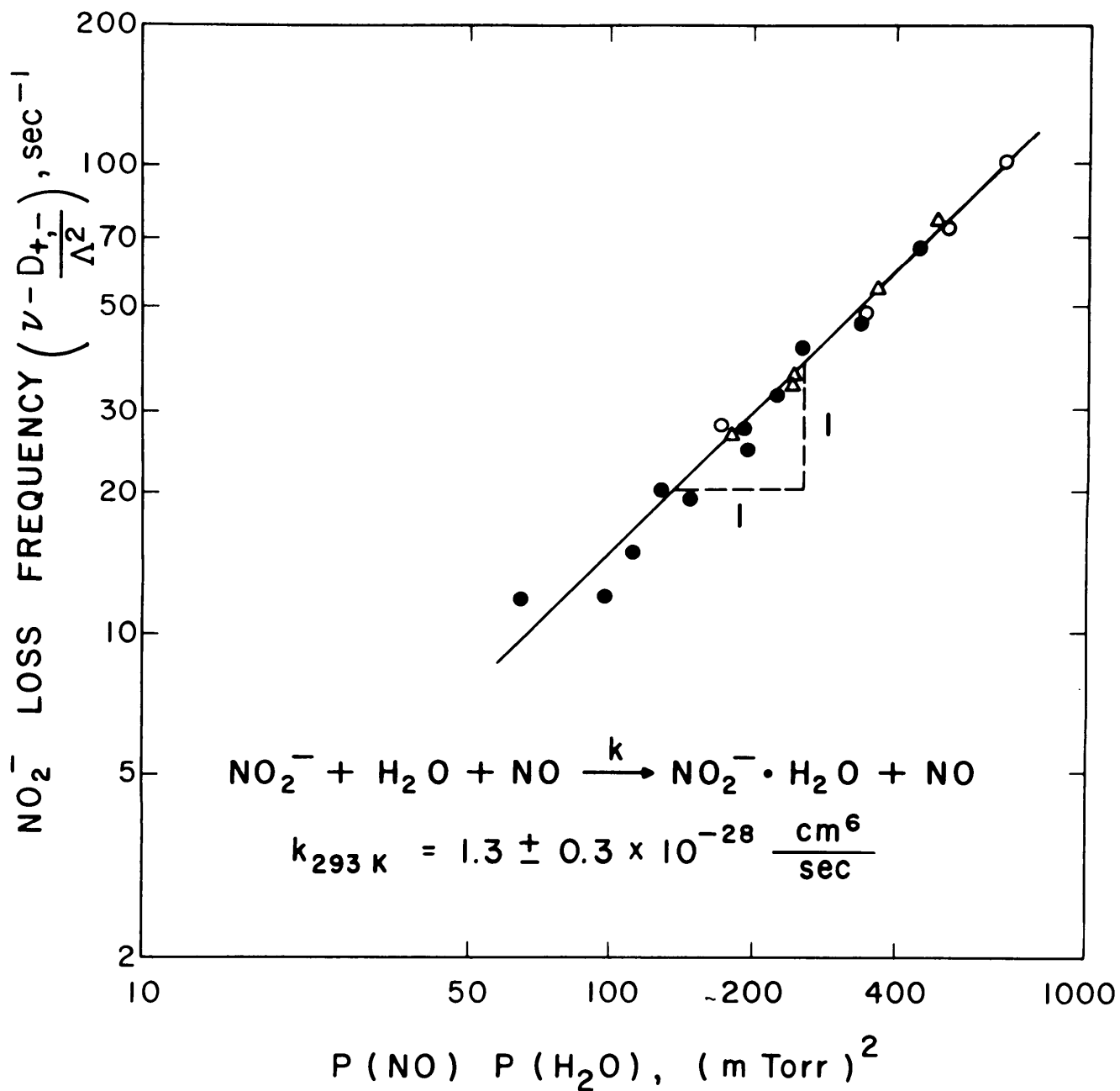


Figure 4. Variation of NO_2^- reactive loss frequency as a function of the product of NO and H_2O pressures

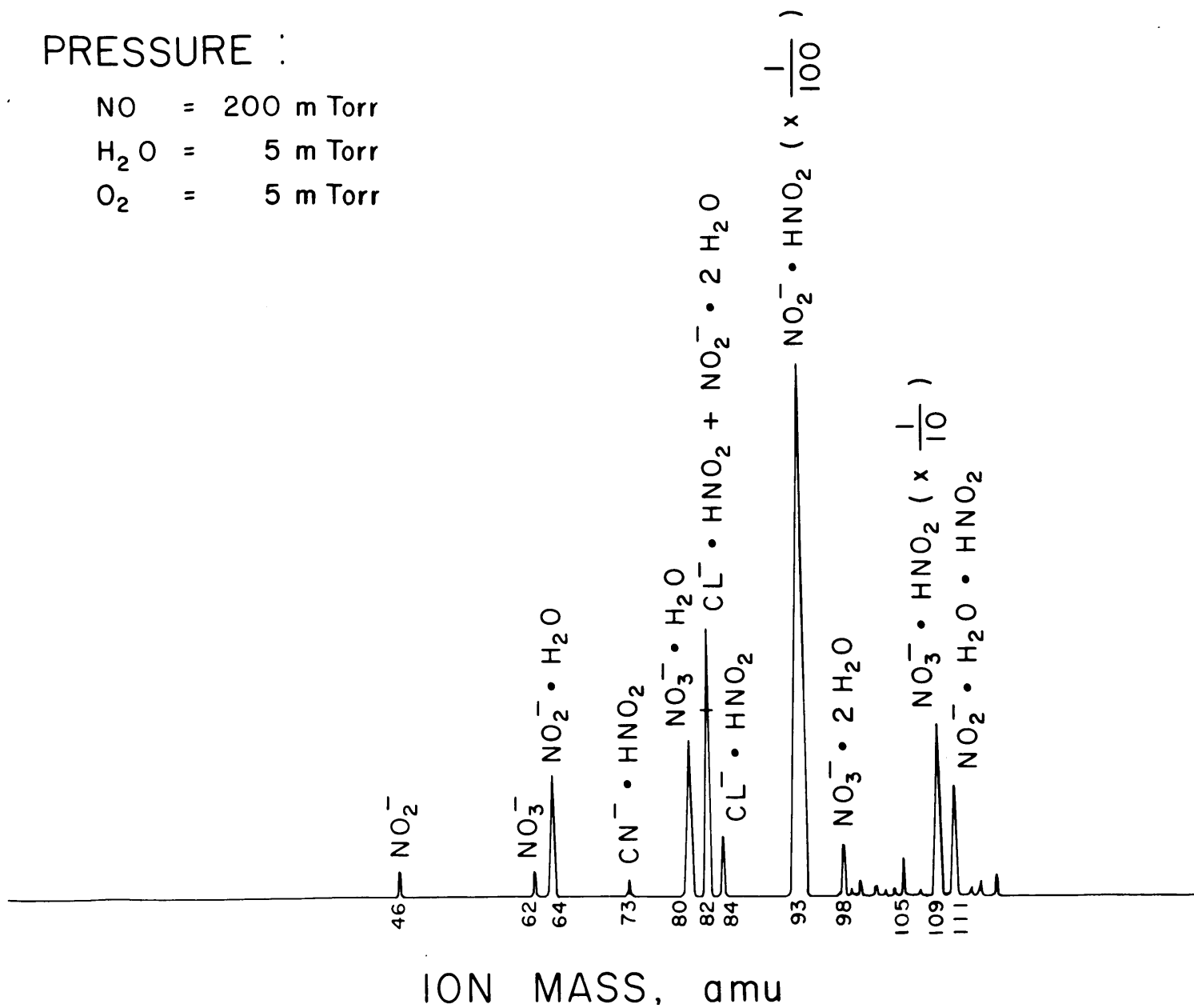


Figure 5. Negative ion spectrum in 200 mTorr NO, 5 mTorr H₂O and 5 mTorr O₂

will certainly be hydrated, and perhaps clustering reactions with other D-region constituents will also be observed.

ACKNOWLEDGEMENTS

The authors have profited from many stimulating discussions of the plasma transition with Dr. M. D. Kregel. M. W. Teague assisted in acquisition and interpretation of much of the experimental data. Appreciation is due Dr. F. E. Niles and Dr. G. E. Keller for numerous discussions concerning experimental results.

REFERENCES

1. W. C. Lineberger and L. J. Puckett, "Positive Ions in Nitric Oxide Afterglows", Phys. Rev., to be published Oct. 1969.
2. W. C. Lineberger and L. J. Puckett, "Hydrated Positive Ions in Nitric Oxide-Water Afterglows", Phys. Rev., to be published.
3. E. E. Ferguson, Rev. Geophys., 5, 305 (1967).
4. R. E. Lelevier and L. M. Branscomb, J. Geophys. Res., 73, 27 (1968).
5. L. J. Puckett, M. W. Teague and D. G. McCoy, "Refrigerating Vapor Bath", Rev. Sci. Instr. submitted for publication.
6. W. L. Fite and J. A. Rutherford, Faraday Soc. Discussions, 37, 192 (1964).
7. H. J. Oskam, Phillips Res. Rpt., 13, 401 (1958).
8. M. D. Kregel, "Diffusion in Decaying Plasmas", J. Appl. Phys., to be published.
9. N. G. Adams, K. K. Bohme, D. B. Dunkin, F. C. Fehsenfeld, and E. E. Ferguson, "Flowing Afterglow Studies of Formation and Reactions of Cluster Ions of O_2^+ , O_2^- and O^- ", J. Chem. Phys., to be published.

DISTRIBUTION LIST

<u>No. of Copies</u>	<u>Organization</u>	<u>No. of Copies</u>	<u>Organization</u>
20	Commander Defense Documentation Center ATTN: TIPCR Cameron Station Alexandria, Virginia 22314	1	Commanding Officer U. S. Army Mobility Equipment Research & Development Center ATTN: Tech Docu Cen, Bldg 315 Fort Belvoir, Virginia 22060
1	Director Advanced Research Projects Agency ATTN: Dr. D. Mann Department of Defense Washington, D. C. 20301	1	Office of Vice Chief of Staff ATTN: CSAVCS-W-TIS Department of the Army Washington, D. C. 20310
1	Institute for Defense Analyses ATTN: Dr. E. Bauer 400 Army-Navy Drive Arlington, Virginia 22202	1	Commanding Officer U. S. Army Research Office (Durham) ATTN: Dr. Robert Mace Box CM, Duke Station Durham, North Carolina 27706
1	Director Defense Atomic Support Agency ATTN: STRA (RAEL) Dr. C. A. Blank Washington, D. C. 20305	3	Commander U. S. Naval Air Systems Command ATTN: AIR-604 Washington, D. C. 20360
1	DASA Information and Analysis Center TEMPO, General Electric Company ATTN: Dr. D. Griesinger 816 State Street Santa Barbara, California 93102	3	Commander U. S. Naval Ordnance Systems Command ATTN: ORD-9132 Washington, D. C. 20360
1	Commanding General U. S. Army Materiel Command ATTN: AMCRD-TE Washington, D. C. 20315	1	AFWL (WLREH, CPT Greene) Kirtland AFB New Mexico 87117
1	Commanding General U. S. Army Materiel Command ATTN: AMCRD-BN, Mr. N. Stulman Washington, D. C. 20315	6	AFCRL (CRUB, Dr. Keneshea, Dr. Hunt, Dr. Champion, Dr. Paulson, Dr. Murad; CRUS, Dr. Huffman) L. G. Hanscom Field Bedford, Massachusetts 01731
1	Commanding General U. S. Army Materiel Command ATTN: AMCRD-TP Washington, D. C. 20315	2	Director National Bureau of Standards ATTN: Dr. L. Kieffer Dr. S. Smith Washington, D. C. 20234

DISTRIBUTION LIST

<u>No. of Copies</u>	<u>Organization</u>	<u>No. of Copies</u>	<u>Organization</u>
8	Director Environmental Science Services Administration ATTN: Div 540.00, Dr. Fehsenfeld Dr. E. Ferguson Div 540.30, Dr. Albritton Dr. Schmeltekopf Div 224.00, Dr. G. Dunn Dr. W. C. Lineberger U. S. Department of Commerce Boulder, Colorado 80302	3	Lockheed Missiles and Space Company ATTN: Dr. R. Gunton Dr. R. Meyerott Dr. R. Varney 3251 Hanover Street Palo Alto, California 94304
1	AVCO-Everett Research Laboratory ATTN: Dr. E. Sutton 2385 Revere Beach Parkway Everett, Massachusetts 02149	1	Midwest Research Institute ATTN: Dr. T. A. Milne Kansas City, Missouri 64110
1	G. C. Dewey Corporation ATTN: Dr. M. Hirsh 202 East 44th Street New York, New York 10017	1	Pennsylvania State University Ionosphere Research Laboratory Electrical Engineering East ATTN: Dr. M. F. Zabielski University Park, Pennsylvania 16802
3	Gulf General Atomic ATTN: Dr. J. McGowan Dr. B. Turner Mr. J. Rutherford P. O. Box 608 San Diego, California 92112	1	The Rand Corporation ATTN: Dr. F. Gilmore 1700 Main Street Santa Monica, California 90406
2	General Electric Company Space Science Laboratory ATTN: Dr. M. Bortner Dr. R. Kummner P. O. Box 8555 Philadelphia, Pennsylvania 19101	2	Sandia Corporation ATTN: Dr. B. Long, Jr. Dr. G. Tisone P. O. Box 5800 Albuquerque, New Mexico 87115
3	Georgia Institute of Technology Physics Department ATTN: Dr. D. Martin Dr. E. McDaniel Dr. E. Thomas Atlanta, Georgia 30332	2	Southwest Center for Advanced Studies ATTN: Dr. C. Collins Dr. W. Hart P. O. Box 30365 Dallas, Texas 75230
		2	Stanford Research Institute ATTN: Dr. I. Poppoff Dr. F. Smith 333 Ravenswood Avenue Menlo Park, California 94025

DISTRIBUTION LIST

<u>No. of Copies</u>	<u>Organization</u>
1	University of Delaware Department of Physics ATTN: Dr. S. B. Woo Newark, Delaware 19711
2	University of Illinois Aeronomy Laboratory ATTN: Dr. C. Sechrist, Jr. Dr. S. Bowhill Urbana, Illinois 61801
4	University of Pittsburgh Cathedral of Learning ATTN: Prof. M. Biondi Prof. W. Fite Prof. F. Kaufman Dr. E. Zipf Pittsburgh, Pennsylvania 15213
2	University of Washington Department of Physics ATTN: Dr. R. Geballe Dr. K. Clark Seattle, Washington 98105

Aberdeen Proving Ground

Ch, Tech Lib
Marine Corps Ln Ofc
CDC Ln Ofc

DOCUMENT CONTROL DATA - R & D

(Security classification of title, body of abstract and indexing annotation must be entered when the overall report is classified)

1. ORIGINATING ACTIVITY (Corporate author) U. S. Army Aberdeen Research and Development Center Ballistic Research Laboratories Aberdeen Proving Ground, Maryland 21005		2a. REPORT SECURITY CLASSIFICATION UNCLASSIFIED	
		2b. GROUP	
3. REPORT TITLE NEGATIVE ION REACTIONS IN NO-H ₂ O MIXTURES			
4. DESCRIPTIVE NOTES (Type of report and Inclusive dates)			
5. AUTHOR(S) (First name, middle initial, last name) Lawrence J. Puckett and William C. Lineberger			
6. REPORT DATE December 1969		7a. TOTAL NO. OF PAGES 29	7b. NO. OF REFS 9
8a. CONTRACT OR GRANT NO.		9a. ORIGINATOR'S REPORT NUMBER(S) Report No. 1463	
b. PROJECT NO. RDT&E 5910.21.61160			
c.		9b. OTHER REPORT NO(S) (Any other numbers that may be assigned this report)	
d.			
10. DISTRIBUTION STATEMENT This document has been approved for public release and sale; its distribution is unlimited.			
11. SUPPLEMENTARY NOTES		12. SPONSORING MILITARY ACTIVITY U. S. Army Materiel Command Washington, C. C.	
13. ABSTRACT A stationary afterglow system has been utilized to determine rate constants for thermal energy negative ion-molecule reactions in photoionized NO-H ₂ O mixtures. When the decay of the plasma is controlled by ambipolar diffusion of positive and negative ions quantitative determination of rate constants is shown to be feasible. The plasma transition from electron-positive ion ambipolar diffusive domination of the transport loss processes to domination by positive ion-negative ion ambipolar diffusion is explained by a model which includes the effects of negative ion trapping. Prominent negative ions in the afterglow include NO ₂ ⁻ , its hydrates, and clusters involving HNO ₂ . Reaction rate constants for the processes $\text{NO}_2^- + \text{H}_2\text{O} + \text{NO} \rightarrow \text{NO}_2^- \cdot \text{H}_2\text{O} + \text{NO}$ $\text{Cl}^- + \text{H}_2\text{O} + \text{NO} \rightarrow \text{Cl}^- \cdot \text{H}_2\text{O} + \text{NO}$ are found to be $1.3 \pm 0.3 \times 10^{-28} \text{ cm}^6/\text{sec}$ and $3.4 \pm 1.3 \times 10^{-29} \text{ cm}^6/\text{sec}$ at 293 K, respectively. Steady glows in NO-H ₂ O-O ₂ mixtures revealed that NO ₂ ⁻ and the impurity HCO ₃ ⁻ also formed multiple hydrates and clustered with HNO ₂ . These results indicate that the terminal negative ions in the D-region of the ionosphere will likely be hydrated.			

14. KEY WORDS	LINK A		LINK B		LINK C	
	ROLE	WT	ROLE	WT	ROLE	WT
Afterglows Nitric Oxide Hydrated Ions Hydronium Ions Chemical Reactions Reaction Rate Constants Clustered Ions Photoionization Negative Ions Ambipolar Diffusion Ionospheric Chemistry						